

Temperature Modulation of Slow and Fast Cortical Rhythms

R. Reig,¹ M. Mattia,⁴ A. Compte,¹ C. Belmonte,³ and M. V. Sanchez-Vives^{1,2}

¹Institut d'Investigacions Biomèdiques August Pi i Sunyer; ²Institució Catalana de Recerca i Estudis Avançats, Barcelona; ³Instituto de Neurociencias de Alicante, Universidad Miguel Hernández, Consejo Superior de Investigaciones Científicas, San Juan de Alicante, Spain; and ⁴Istituto Superiore di Sanità, Rome, Italy

Submitted 11 November 2009; accepted in final form 22 December 2009

Reig R, Mattia M, Compte A, Belmonte C, Sanchez-Vives MV. Temperature modulation of slow and fast cortical rhythms. *J Neurophysiol* 103: 1253–1261, 2010. First published December 23, 2009; doi:10.1152/jn.00890.2009. In the local cortical network, spontaneous emergent activity self-organizes in rhythmic patterns. These rhythms include a slow one (<1 Hz), consisting in alternation of up and down states, and also faster rhythms (10–80 Hz) generated during up states. Varying the temperature in the bath between 26 and 41°C resulted in a strong modulation of the emergent network activity. Up states became shorter for warmer temperatures and longer with cooling, whereas down states were shortest at physiological (36–37°C) temperature. The firing rate during up states was robustly modulated by temperature, increasing with higher temperatures. The sparse firing rate during down states hardly varied with temperature, thus resulting in a progressive merging of up and down states for temperatures around 30°C. Below 30°C and down to 26°C the firing lost rhythmicity, becoming progressively continuous. The slope of the down-to-up transitions, which reflects the speed of recruitment of the local network, was progressively steeper for higher temperatures, whereas wave-propagation speed exhibited only a moderate increase. Fast rhythms were particularly sensitive to temperature. Broadband high-frequency fluctuations in the local field potential were maximal for recordings at 36–38°C. Overall, we found that maintaining cortical slices at physiological temperature is critical for the generated activity to be analogous to that in vivo. We also demonstrate that changes in activity with temperature were not secondary to oxygenation changes. Temperature variation sets the in vitro cortical network at different functional regimes, allowing the exploration of network activity generation and control mechanisms.

INTRODUCTION

Temperature is a crucial parameter in homeostasis and its effects on different parameters of neural activity have been measured since the early days of electrophysiology. At the cellular level, changes in temperature affect membrane potential, input resistance, action potential amplitude, duration and propagation, and ionic currents (Borst and Sakmann 1998; Hodgkin and Katz 1949; Thompson et al. 1985; Volgushev et al. 2000b). Synaptic transmission is also affected by changes in temperature, both in invertebrates and mammals (Fujii et al. 2002; Kullmann and Asztely 1998; Thompson et al. 1985; Volgushev et al. 2000a). The sensitivity of synaptic transmission to temperature is such that changes in brain temperature associated with physiological conditions (warming up of arterial blood with muscle exercise, lowering of temperature during swimming) are enough to modify the amplitude of synaptic potentials in the hippocampus (Andersen and Moser 1995; Moser et al. 1993).

Address for reprint requests and other correspondence: M. V. Sanchez-Vives, IDIBAPS, Villarroel, 170, 08036 Barcelona, Spain (E-mail: msanche3@clinic.ub.es).

With a major impact on the properties of individual neurons and on synaptic transmission, it is evident that temperature must have a great effect on network activity. Lowering temperature has been reported to decrease synchronization in the hippocampal network (Javedan et al. 2002; Motamedi et al. 2006) and, for that reason, it has been used to decrease epileptic activity (Rothman 2009; Rothman et al. 2005). On the contrary, higher temperatures increase gamma synchronization in the hippocampus (Wu et al. 2001). Furthermore, metabolic processes are temperature dependent (Esmann and Skou 1988) and it is for this that cooling of the cortex is also a common strategy to decrease the activity of cortical or other brain areas to determine their function (Schiller et al. 1974). This strategy induces hyperexcitability while at 18–24°C and thus neighboring areas of the cooled down network may have their excitability increased (Volgushev et al. 2000a).

Here we studied how systematically changing temperature between 30 and 41°C affects emergent activity in the cerebral cortex in vitro. As occurs in vivo (Steriade et al. 1993, 1996), cortical slices maintained at physiological temperatures generate a slow rhythm consisting in up and down states (Sanchez-Vives and McCormick 2000), whereas faster rhythms (beta, gamma) have also been reported during up states (Compte et al. 2008). We find that both network-generated activities (slow and fast rhythms) are exquisitely sensitive to temperature. This is relevant to explain differences in the emergent activity between different preparations, laboratories, or between in vivo and in vitro conditions, as well as during situations of increased temperature such as periods of fever or physical exercise (Moser et al. 1993). Furthermore, we propose that the modulation of network activity exerted by temperature is also an interesting model to explore which mechanisms may be involved in the control of cortical activity, since varying temperature sets the network at different functional regimes.

METHODS

Slice recordings

In vitro experiments were performed on cortical slices from 4- to 10-mo-old ferrets of either sex that were deeply anesthetized with sodium pentobarbital (40 mg/kg) and decapitated. Their brains were quickly removed and placed in ice-cold cutting solution. Ferrets were cared for and used in accordance with the European Union guidelines on protection of vertebrates used for experimentation (Strasbourg 3/18/1986) as well as approved by the local ethical committee.

Coronal slices (thickness: 400 μ m) of the primary visual cortex were cut on a vibratome. A modification of the technique developed by Aghajanian and Rasmussen (1989) was used to increase tissue viability. After preparation, slices were placed in an interface-style recording chamber (Fine Science Tools, Foster City, CA) and bathed

in artificial cerebrospinal fluid (ACSF) containing (in mM): NaCl, 124; KCl, 2.5; MgSO₄, 2; NaHPO₄, 1.25; CaCl₂, 2; NaHCO₃, 26; and dextrose, 10 and was aerated with 95% O₂-5% CO₂ to a final pH of 7.4. Bath temperature was initially maintained at 34–35°C. After a 2-h recovery, the ACSF was replaced by “in vivo like” ACSF containing KCl, 3.5; MgSO₄, 1; CaCl₂, 1; the remaining components were the same as those just described. Extracellular, unfiltered recordings were obtained by means of tungsten electrodes through a Neurolog system (Digitimer) amplifier. Recordings were digitized, acquired, and analyzed using a data acquisition interface and software from Cambridge Electronic Design (Cambridge, UK).

Temperature control

Temperature was modified in ramps starting from 34 to 35°C. The temperature of the ACSF entering the recording chamber (Fine Science Tools) was modified by controlling the temperature of the water bath surrounding the recording chamber. The temperature controller (Fine Science Tools) regulates a heating blanket immersed in the water bath, which then induces warming up (or not) of the ACSF circulating in a tube through the water bath. The desired temperature is set in the controller and, once the temperature has been reached, the power to the heating blanket stops. That is a slow procedure and usually changing one degree takes a minimum time of 5 min. The thermistor used to measure the temperature is located at the bottom of the recording chamber. The temperature in the bottom of the recording chamber (where the thermistor is located) differed from that measured at the level of slices by 0.2°C. Increasing (toward 41°C) or decreasing ramps (down to 30°C and in four occasions to 26°C) were given, usually covering the whole temperature range between 30 and 41°C.

Oxygen levels at different temperatures

As mentioned earlier, the experiments presented here were carried out in an interface-style recording chamber, where oxygen reaches the slice both dissolved in the ACSF (aerated with carbogen, 95% O₂-5% CO₂ gas mixture) and mainly by diffusion from the humidified and oxygen-rich air surrounding the slice. For that purpose, the warm water compartment below the recording chamber is also aerated with carbogen. Local oxygen level is a critical factor for the generation and propagation of network activity (Hajos et al. 2009) and we checked that the effects of increasing temperature on the slice activity was not secondary to oxygen deprivation. Oxygen was measured with an optode (tip diameter: 50 μm; Microx TX3, PreSens, Regensburg, Germany) during ramps of temperature between 28 and 42°C (Fig. 1; Supplemental Fig. S1).¹ This microsensor is designed and was calibrated to be used in liquid, tissue (response time: 1 s), and air (response time: 0.5 s). Oxygen in the air around the slice was of 90% at 28°C and dropped to 85% at 42°C. Next, we measured oxygen levels in the ACSF in which the slice was bathed. Oxygen levels were of 66% at 28°C and dropped to 60% when at 42°C. Oxygen level was also measured in layer 5 of visual cortex slices ($n = 3$) at about 100-μm depth during a temperature ramp (28–42°C). In two of these three slices, concurrent spontaneous activity was recorded (Supplemental Fig. S1). While at 30°C the oxygen level in an active slice was of 65.5–66.5% ($n = 3$) and decayed progressively while increasing the temperature, reaching 59–61% while at 42°C. Note that the oxygen level in our interface-style chamber while at 42°C is the same as that recorded in an optimized submerged-style chamber while at 32°C (Hajos et al. 2009). We conclude from these measurements that the effects of temperature changes described in this study are not due to changes in the oxygenation of the tissue. Furthermore, the activity changes induced by hypoxia that we describe in Supplemental Fig. S1 differ from those observed for temperatures >36°C.

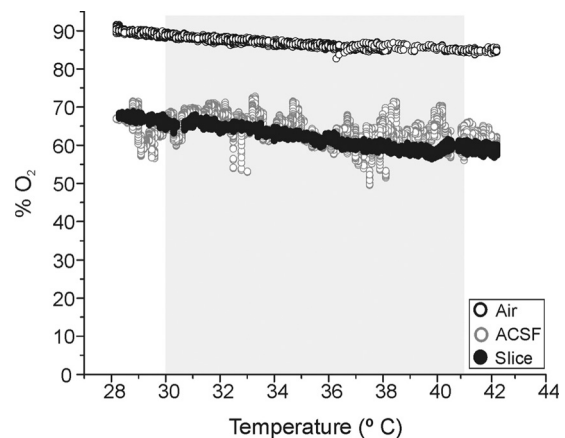


FIG. 1. Oxygen levels at different temperatures. Cortical slices were recorded from in an interface-style chamber and oxygen levels were measured with an optode (tip diameter, 50 μm; Microx TX3). The percentage of oxygen in the air surrounding the slice (black, empty circles), artificial cerebrospinal fluid (ACSF, gray, empty circles), and in layer 5 of an active visual cortex slice (black circles) are represented for a ramp of temperatures between 28 and 42°C. The complete ramp took 90 min. Each symbol corresponds to 1 s. The larger variability in the measurements taken in the ACSF are probably due to the flow dynamics. The gray background shows the temperature range for most of the experimental results (30–41°C).

Data analysis

Multiunit activity (MUA) was estimated as the power change in the Fourier components at high frequencies (>200 Hz) of the extracellular recordings. High-frequency components of the extracellular recording can be seen as a linear transform of the instantaneous firing rate of the neurons surrounding the electrode tip. Theoretical studies show that the normalized MUA spectrum provides a good estimate of the population firing rate, given that normalized Fourier components at high frequencies have densities proportional to the spiking activity of the involved neurons (Mattia and Del Giudice 2002). The power spectra of the extracellular recording were computed every 5 ms and their average during down states, $36 \pm 1^\circ\text{C}$, was chosen as baseline for normalization. The time-dependent MUAs were the average power of the normalized spectra in the frequency band 0.2–1.5 kHz (Fig. 2A). With respect to a similar approach in Stark and Abeles (2007), the preceding estimate provides a larger signal-to-noise ratio: using normalized spectra the components at different frequencies have similar orders of magnitude and averaging across the very high frequency band (0.2–1.5 kHz) improved the MUA estimate. MUAs were logarithmically scaled to balance the large fluctuations of the nearby spikes. Furthermore, log (MUA) time series were smoothed by a moving average with a sliding window of 80 ms. For each recording and temperature range, log (MUA) was further shifted to have a zero value for the minimum level of the average activity following the detected up-to-down transitions. This calibration made the spectral estimate of MUA even more insensitive to possible slow varying sources of background noise and allowed us to estimate population activity during up states in an independent way from activity during down states. This would be otherwise difficult to achieve by estimating the activity from the height of the central peak of the autocorrelation (AC), which detects the increment of the firing in the up with respect to the down states. We refer to the spectral estimated log (MUA) in the figures and the remainder of this study as “relative firing rate,” since it is a relative measure resulting from an average of power spectra ratios.

Up and down states were singled out by setting a threshold in the log (MUA) time series (Fig. 2A). The histograms of log (MUA) were bimodal and the positions of the high and low peaks were used as reference activity for up and down states, respectively (Fig. 2D). The discriminating threshold was set to 60% of the interval between the peaks. The lower peak was estimated as the center of Gaussian

¹ The online version of this article contains supplemental data.

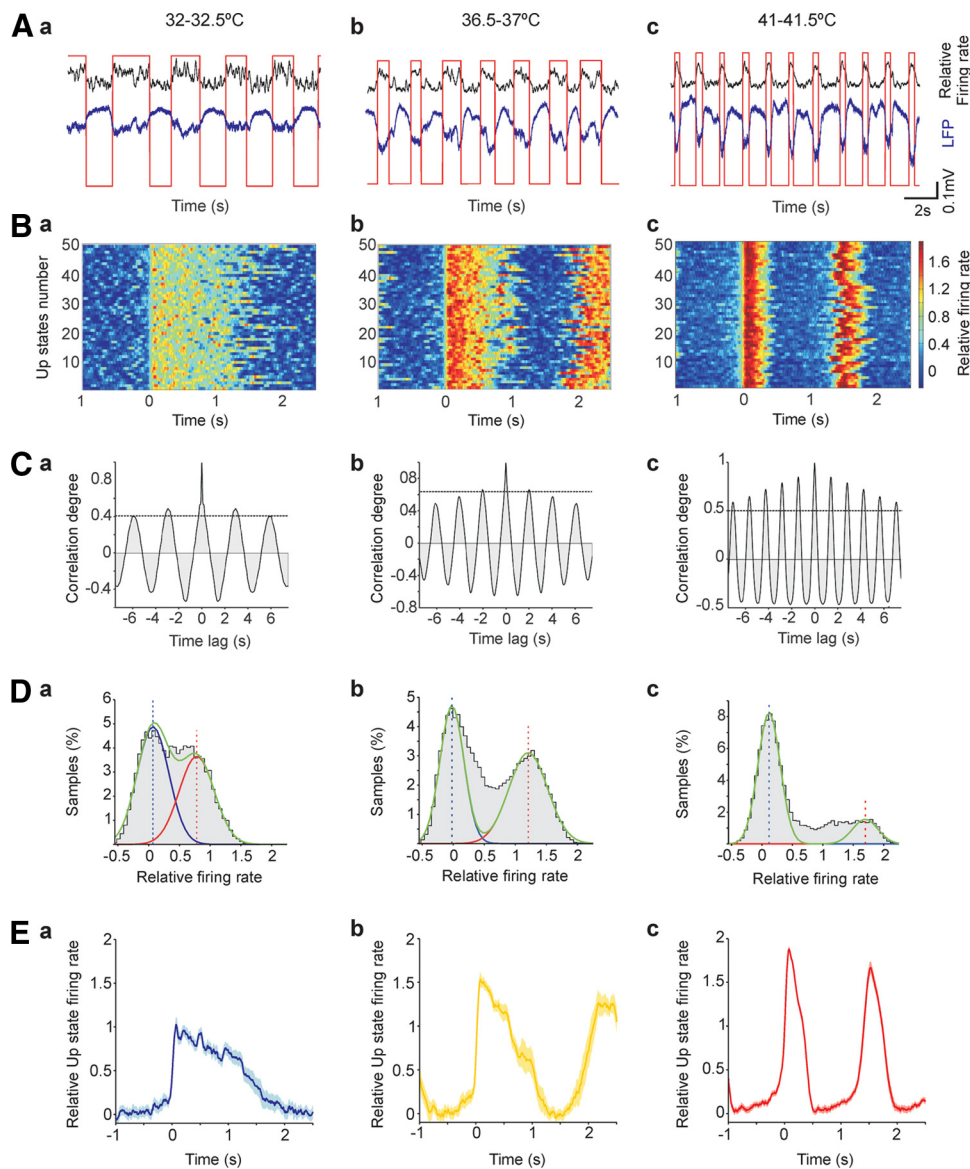


FIG. 2. Quantification methods of oscillatory activity in the cortical network at different temperatures. *A*: slow oscillations in the unfiltered extracellular recording (*bottom*: blue) and in the estimated relative firing rate (*top*: black; see METHODS) using arbitrary units. Red squares show up and down states singled out from relative firing rates. *B*: raster plots display in each row the color-coded time courses of relative firing rates centered around the detected up state onsets in the specific temperature interval. *C*: autocorrelations of the relative firing rates. Horizontal dotted lines are 2-fold the SD of the time series. *D*: histograms of relative firing rate. Red and blue curves are the Gaussian best fits of the upper and lower distribution tails, respectively, aiming at representing the activity distribution during up and down states. The sum of the fitted curves is shown in green. Vertical dotted lines are the averages of the fitted Gaussians. *E*: average relative firing rates across detected up states and centered around down to up state transitions, as in raster plots of *B*. Shaded strips are the related SEs. In all panels, the *left* (*a*), *central* (*b*) and *right* (*c*) columns correspond to different temperature intervals (32–32.5, 36.5–37, and 41–41.5°C, respectively).

distributions fitting the lower tail before the first peak. The tail following the higher peak resulting from the difference of the original histogram with the previously fitted distribution is furthermore fitted by a second Gaussian distribution whose center was used as the position of the high activity peak. To remove the effects of small activity fluctuations a cutoff in the minimum state duration was set in a range $[1/3, 1/2]$ of the average up-state length. This lower limit was chosen case by case to reproduce the up/down oscillation frequency estimated from the log (MUA) autocorrelation. Small periods were recursively removed, converting short up (down) states in longer down (up) states. Finally, times of transition between states were better estimated by fitting the log (MUA) in a 100-ms window around the transitions with third-degree polynomials. The adjusted transition was set to the crossing time of the polynomial with the discriminating threshold.

The “relative firing rate” in the up state for a given temperature range was estimated as the maximum average log (MUA), centered around up-state onset, in the 300 ms following the transition. The average down activity was the average log (MUA) in the time series subset labeled as down states. The slopes of the upward transitions were the gradients of the linear fits of the average log (MUA) in the time interval $(-10, 25)$ ms around the up-state onset. Similarly, the slopes of the downward transitions were from the linear fits of

log (MUA) centered around up-to-down transitions in the time interval $(-25, 10)$ ms.

For the analysis of high-frequency synchronization in the local field potential (LFP), we applied the same analysis protocols as described previously (Compte et al. 2008). In brief, we obtained the LFP signal by low-pass filtering the extracellular recording at 150 Hz. Then, 0.5-s periods of large-amplitude fluctuations in the LFP were selected as up states and their spectral content was evaluated with a multitaper spectral estimate. This yielded a power spectrum of up state LFP activity characterizing the corresponding temperature regime. Two measures were extracted from such power spectra: average power and relative average power in the 15- to 40-Hz band. The average power gave an indication of how the amplitude of gamma-band fluctuations was affected by temperature. The relative average power, obtained by dividing the average gamma-range power by the average spectral power over the whole frequency range (5–100 Hz), provided a view of how frequency-band selective the change in power was with temperature. A strong modulation in average power without significant modulation in relative average power was indicative that temperature-dependent modulations were not systematically affecting a particular frequency band, but operated modulating nonselectively LFP fluctuations.

All off-line analyses were implemented in MATLAB (The MathWorks, Natick, MA).

RESULTS

The activity generated spontaneously by slices of ferret visual cortex was recorded while the temperature in the bath was gradually modified between 30 and 41°C ($n = 21$) and in four cases from 26°C. Twenty to 30 min after switching from classical ACSF to “in vivo-like” ACSF, and at 36°C, spontaneous slow rhythmic activity appeared in the slice as described in Sanchez-Vives and McCormick (2000) (Fig. 2). This activity consisted of the alternation between up and down states and is reminiscent of the activity that is generated in the cortex in vivo during slow-wave sleep (Steriade et al. 1993). The occurrence of this activity was recorded as an unfiltered (0.1 Hz to 5 kHz) extracellular recording by means of tungsten electrodes, where up states appeared as negative deflections (Fig. 2A). The temperature of the ACSF was then modified in increasing or decreasing ramps (see METHODS). In all cases, temperature changes were carried out slowly (≥ 5 min/deg), which provided long recordings per temperature level (between 30 and 200 up states were averaged per degree).

We performed our analyses on two distinct signals derived from our extracellular recordings: spiking activity was studied in high-frequency (0.2–1.5 kHz) components, whereas network rhythmicity and fluctuations in synaptic activity were evaluated from the LFP in the low-frequency band (<100 Hz).

Neural spiking analysis was done both on the transformed high-pass-filtered extracellular record, which we will refer to as “relative firing rate” or simply “firing rate” (see METHODS) and on its autocorrelograms (Fig. 2, A and C), resulting in similar findings.

An example of transformation of cortical rhythmic activity with temperature

Figure 2 illustrates a full representative example of the transformation of the rhythmic spontaneous activity induced by temperature. In this case the emergent activity was evaluated at three points of the temperature ramp: 32, 36, and 41°C. The activity observed at 36°C (Fig. 2, *middle column*) is representative of the physiological one (Fig. 2*Ab*). This physiological activity is also illustrated in the raster plots (Fig. 2*Bb*), where successive up states were aligned at *time 0* and the color scale represents firing rate. Up states at physiological temperature occurred at an average frequency of 0.38 Hz, as illustrated in the autocorrelogram (Fig. 2*Cb*). The histograms of firing rate values show a bimodal distribution that corresponds to up and down states (Fig. 2*Db*). The average profile of the network firing rate during up states is shown in Fig. 2*Eb*, where the shadow is the SE.

The pattern of rhythmic activity generated by the network was contingent on temperature. When temperature was lowered (32°C in Fig. 2, *left column*), the duration of the up states increased—in this case by almost twofold—while the firing rate during up states decreased (Fig. 2, *Ba* and *Ea*) and the frequency of occurrence of up states decreased. On the other hand, increasing the temperature (to 41°C in Fig. 2, *right column*) resulted in opposite changes: shorter and more frequent up states and higher firing rates during up

states (Fig. 2, *Cc–Ec*). Further analysis of the case displayed in Fig. 2 is presented in Supplemental Fig. S2, in which the average firing rate during slow oscillation cycles and their SEs are represented for seven different temperatures to illustrate the progressive change of the oscillatory cycles with temperature, as well as the histograms of up-state (red) and down-state (blue) durations at these seven different bath temperatures.

Transformation of oscillatory cycle and firing rate with temperature in the population

All the modifications on rhythmic activity due to temperature described so far for a single case occurred in the same direction in the whole population ($n = 16$, Figs. 3 and 4). The average absolute frequency of up states increased progressively between 32 (0.22 Hz) and 36°C (0.37 Hz), remaining in a plateau around 0.34 Hz for higher temperatures (Fig. 3A). However, when the up state frequency was normalized for each slice with respect to that at 36°C, we observed that the relative frequencies reached a maximum at 40°C, gradually decreasing for lower temperatures. This representation better reflects what takes place in individual cases (e.g., Fig. 2), where the frequency generally increases for temperatures above the physiological one.

Up-state duration was maximum at 32°C, decaying monotonically to approximately half the value at 41°C. This was the case for both the averaged absolute values and the normalized ones (Fig. 3B). Down-state duration had a more complex dependence on temperature, being minimal at physiological temperature (36–37°C) and increasing from there toward cooler or warmer temperatures (Fig. 3C). Thus for temperatures <36°C the elongation of both up and down states with coldness results in a progressively lower frequency of the oscillatory cycles.

The firing rate during up states increased significantly from 32 to 39°C, remaining in a plateau for higher temperatures (Fig. 4, A and B). When looking at individual cases, we observed that sometimes a maximum firing rate was reached at 36–39°C, decreasing progressively for higher temperatures (not shown). During down states neuronal firing is sparse (Compte et al. 2003; Shu et al. 2003) and is hardly affected by temperature (Fig. 4C). This stable firing during down states at different temperatures, together with the decrease of firing rate during up states with cooling (Fig. 4B), results in an increase in the down versus up firing rate with cooling (Fig. 4D). While at $\leq 32^\circ\text{C}$, this results in a continuous firing where separation between up and down states is no longer possible. The trend toward merging of up and down states at lower temperatures can be seen in the histograms in Fig. 2D and Supplemental Fig. S3, B–F.

Cooler temperatures (<36°C) were associated with more irregular, noisier slow oscillations, with an increased variability of up and down state durations. The raster plots representing up states in a particular case in Fig. 2 illustrate that the variability of up state duration at 32°C (Fig. 2*Ba*) was greater than that at 41°C (Fig. 2*Bc*). The same was the case for the down state duration; thus the coefficient of variation (CV) of the up and down cycle average duration was significantly increased for lower temperatures in the population (Fig. 4, E and F). The average CV remains in a plateau for temperatures

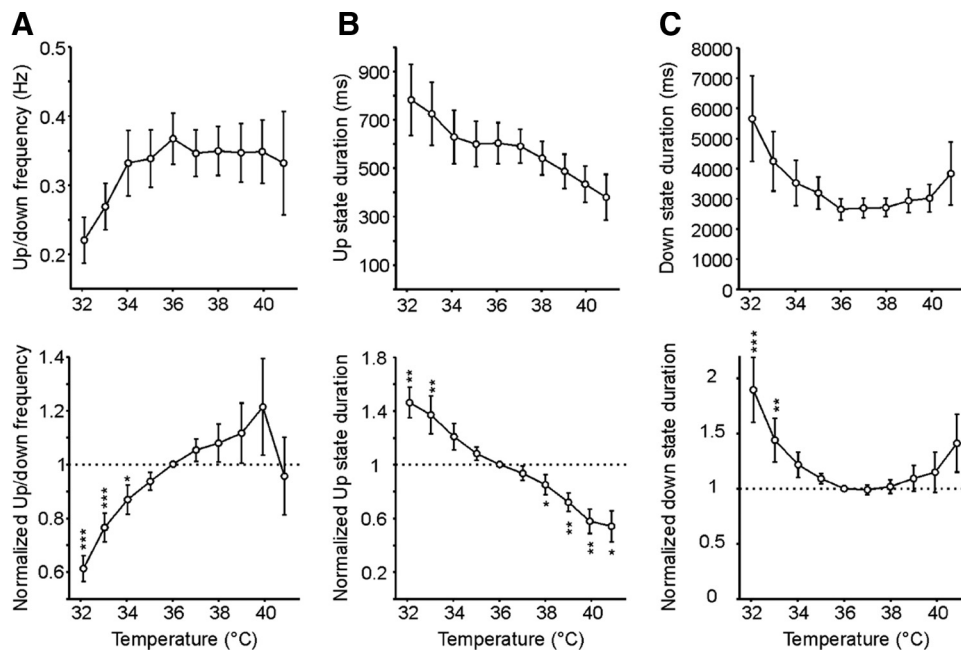


FIG. 3. Variation of oscillatory frequency and up- and down-state durations with temperature. *A*: frequency of occurrence of up and down cycles at different temperatures of the bath. *B*: duration of up states vs. temperature. *C*: duration of down states vs. temperature. In all panels, the *top graphs* correspond to the absolute values and in the *bottom graphs* all the values have been normalized with respect to those at 36°C (dashed line). All points represent the averages of values corresponding to 10–16 slices. Error bars are the SEs. A Wilcoxon signed-rank test was used to evaluate how different the normalized averages were from 1.0. Significance is represented in the graphs as: * $P < 0.05$; ** $P < 0.01$; *** $P < 0.001$.

of $\geq 36^\circ\text{C}$, whereas it increases parametrically for temperatures below the physiological one.

Effect of temperature on down-to-up and up-to-down transitions

The rate of the down to up state transition was also temperature dependent, in general being faster at higher temperatures (Fig. 5, *A* and *B*). This speed was quantified as the slope of the transition of the firing rate (Fig. 5*A*) and it reflects the faster rate of recruitment of the local network during up state onset at higher temperatures. The normalized population values showed a progressive increase in the slope between 32 and 39°C. A similar, although less-pronounced effect, was observed in the up to down transition, which was also faster for higher temperatures (Fig. 5, *C* and *D*). In both cases, a maximum value was reached at 39°C, remaining constant for higher temperatures (Fig. 4, *B* and *C*). The different degree of changes in

up-down versus down-up rate is suggestive of different mechanisms regulating both transitions. The slower up to down and down to up transitions recorded for colder temperatures were related to the progressive merging between up and down state firing while at cooler temperatures (see preceding text).

Effect of temperature on slow oscillation propagation

Next, the speed of wave propagation along the network was measured with two electrodes from layer 5 at a distance of 1–3 mm. Figure 6*A* illustrates the raster plots of up states from two simultaneous recordings (MU1 and MU2) aligned around the down to up transitions detected from electrode 1 in a temperature range of 37–37.5°C. The time elapsed between the take off of the up state at one electrode to the other allowed us to measure the speed of propagation, which was detected for different temperatures in five slices. The distribution of time

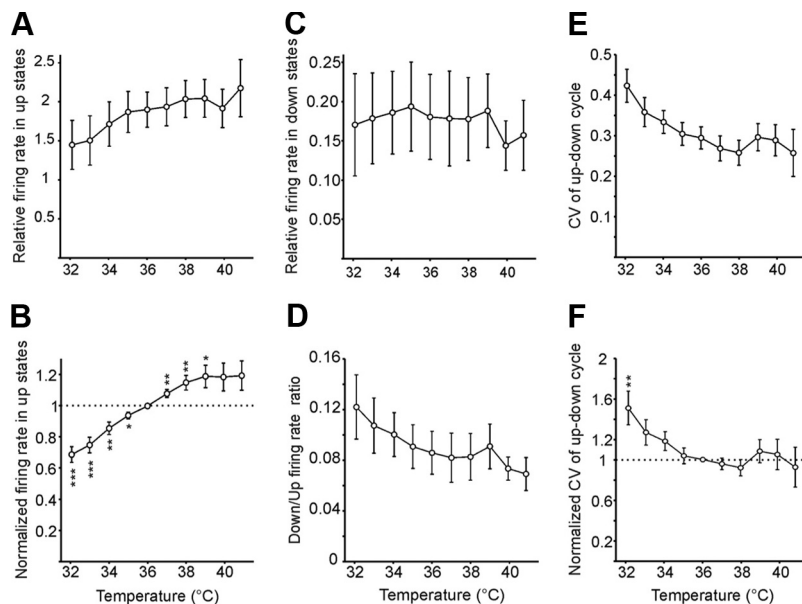


FIG. 4. Variation of firing rate during up and down states and coefficient of variation (CV) of the oscillations with temperature. *A*: relative firing rate during up states vs. temperature. *B*: relative firing rate during up states normalized by that at 36°C. *C*: relative firing rate during down states vs. temperature. *D*: relative firing rate ratio of down/up state at different temperatures. *E*: CV of the duration of up and down cycles vs. temperature. *F*: CV of the duration of up and down cycles normalized by that at 36°C. A Wilcoxon signed-rank test was used to evaluate how different the normalized averages were from 1.0. Significance is represented in the graphs as: * $P < 0.05$; ** $P < 0.01$; *** $P < 0.001$.

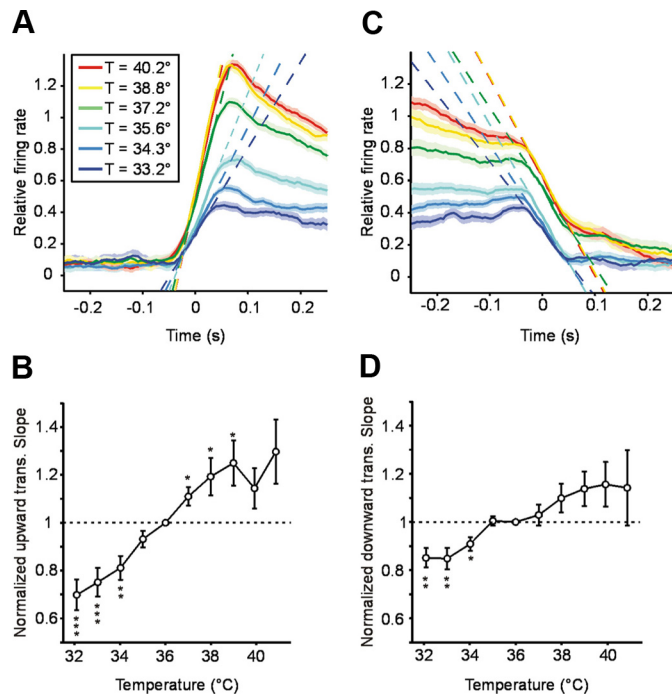


FIG. 5. Temperature dependence of network activation during up and down transitions. *A*: down to up state transition slope. Example of average relative firing rates around down to up transitions at different color-coded temperatures (see *inset*). Dashed lines are linear fits of the activity buildup around the upward transitions (see *METHODS*). *B*: population averages of the slopes of the upward transitions vs. temperature. All values have been normalized with respect to those at 36°C (dashed line) and each point represents the average values for 10–16 cortical slices. *C* and *D*: the same as *A* and *B* but for the up to down transition slope. A Wilcoxon signed-rank test was used to evaluate how different the normalized averages were from 1.0. Significance is represented in the graph as: * $P < 0.05$; ** $P < 0.01$; *** $P < 0.001$.

lags between up states from both electrodes is represented in Fig. 6*B*, where it is shown that while the majority of up states have a delay close to 200 ms between electrode 1 and electrode 2, fewer cases have a similar but negative delay, meaning that there are up states propagating in the opposite direction. The speeds of propagation were estimated considering only the positive branch of the histograms, by averaging the fraction between electrode distance and time lags. Results of speed of propagation for five slices and for different temperatures are represented in Fig. 6*C*, together with the population's linear fit (in black). Three of five cases showed a moderate increase in speed with temperature, whereas the remaining two had a relatively stable speed of propagation independent of temperature. The linear fit for all the estimated speeds shows a trend toward higher speeds for higher temperatures, with a slope of $0.2 \text{ mm} \cdot \text{s}^{-1} \cdot ^\circ\text{C}^{-1}$.

Fast rhythms during up states and temperature

Finally, we estimated the effect of temperature on activity fluctuations in the LFP in the beta/gamma range (15–40 Hz), during up states (Compte et al. 2008). Interestingly, LFP spectral content during up states varied nonmonotonously with temperature, being maximal at physiological temperatures ($\sim 36^\circ\text{C}$, Fig. 7). Typically, LFP spectral enhancement at physiological temperatures was not specific of a frequency band, but occurred globally over frequencies 5–100 Hz (Fig. 7,

A and *B*). This is evidenced by the fact that, in the population ($n = 16$), gamma-range LFP spectral power showed a peak at 36–38°C (Fig. 7*C*, blue), although this peak was absent when the spectrum was normalized to the average power in the whole 5- to 100-Hz range (Fig. 7*C*, green). Thus fast LFP fluctuations during up states were particularly sensitive to temperature. This temperature dependence must be taken into account when studying fast cortical oscillations *in vitro*. Up state LFP fluctuations were amplified nonselectively at physiological temperatures, suggesting that a noisy environment, where synaptic activity fluctuates significantly in the 5- to 100-Hz band, may facilitate cortical processing.

DISCUSSION

In this study we describe the effect that modifying temperature has on the up and down activity that emerges spontaneously in the cortical network *in vitro*. For temperatures ranging between about 26 and 41°C we observed a large range of network behavior expanding from almost continuous firing and absence of up and down states (at lower temperatures) to highly defined up and down states at higher temperatures. Interestingly, high frequencies (10–40 Hz, beta and gamma)

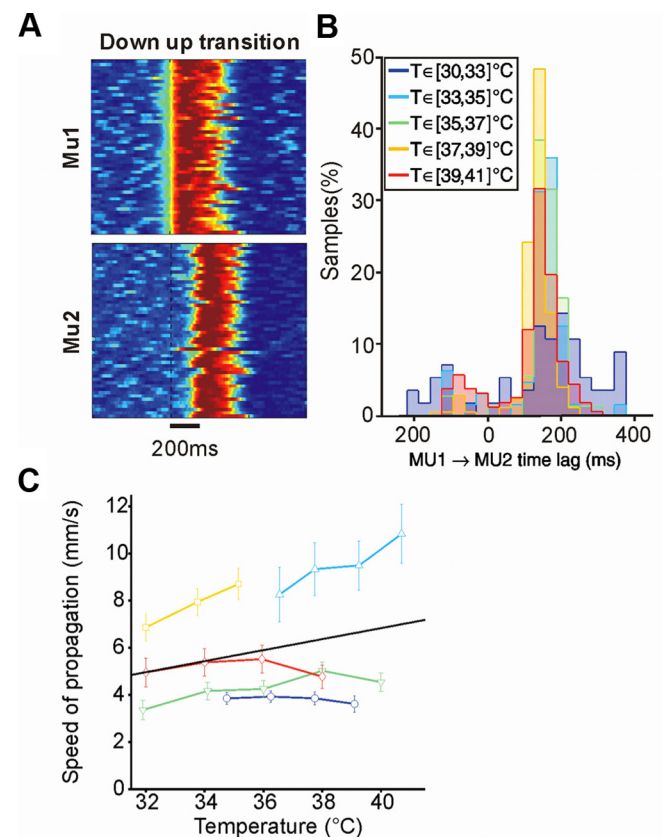


FIG. 6. Temperature dependence of the speed of propagation of up states. *A*: raster plots of color-coded relative firing rate from 2 simultaneous recordings (MU1 and MU2) centered around the occurrence of up states in electrode 1 (MU1). Note that the up states recorded from MU1 are aligned at *time 0*. Fifty-two up states from temperatures between 37 and 37.5°C are detected and displayed in each raster plot. Both electrodes (MU1 and MU2) were separated by $0.71 \pm 0.04 \text{ mm}$. *B*: histograms of the delay of propagation of the traveling waves at different bath temperatures (see *inset*). *C*: average speed of propagation of the wave fronts vs. temperature in 5 cortical slices. The thick black line is the linear fit of the plotted speeds.

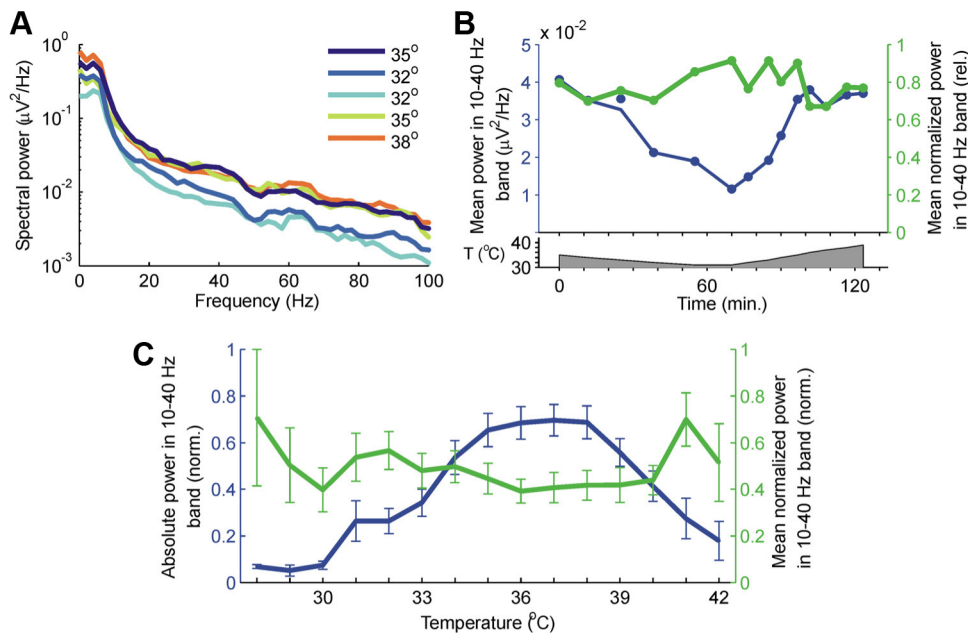


FIG. 7. Local field potential (LFP) fluctuations during up states are temperature dependent. *A*: sample LFP power spectra from up state data in one slice show that temperature nonselectively enhanced LFP spectral power at all frequencies. *B*: quantification of beta/gamma-range (10–40 Hz) spectral power in absolute units (blue) and normalized to the total average power in the range 5–100 Hz (green) for the data in *A*. The *bottom panel* indicates the temperature of the recording as it progressed through the experiment, first decreasing from 35 to 31° and then increasing from 31 to 39°. The lack of modulation in the green curve indicates that spectral modulations were not specific to the beta/gamma range. *C*: averaged results for the population of recordings ($n = 16$). To average across slices, the average power curves (see *B*) were first normalized to their maximal value. Error bars indicate SEs. The flat green curve indicates that the consistent power modulations by temperature were not specific of the 10- to 40-Hz band.

appeared during up states (Compte et al. 2008), showing their maximum power at physiological temperatures (36–38°C). A simultaneous measure of oxygen concentration in the slice while at different temperatures revealed that the effects of temperature on spontaneous activity were not secondary to changes in oxygenation. These results are of interest not only to understand the physiology of the cortical network while varying a relevant parameter of homeostasis, but also to provide a model of cortical network activation that results in different activity regimes of interest to understand the mechanisms controlling up and down states.

At physiological temperature (~36°C) the network exhibited spontaneous up and down states that occurred with a frequency between 0.3 and 0.4 Hz. Temperature variation resulted in a relatively continuous change in a number of parameters including up state duration, frequency, firing rate in up and down states, coefficient of variation of the cycle duration, slope of the transitions, speed of propagation, and fast frequency content in up states.

Temperature affects a large number of processes that are involved in network activity. Some of these factors would induce an increase of activity, others a decrease. Consequently, it is difficult to predict what the changes on cortical emergent activity would be. Lowering temperature increases input resistance of neurons both in the hippocampus (Thompson et al. 1985) and in the cortex (Volgushev et al. 2000b). The membrane potential of cortical neurons becomes more depolarized with cooling, at a rate of -1.03 to -2.21 mV/°C (Volgushev et al. 2000b), whereas it was reported not to change for hippocampal cells (Thompson et al. 1985). No changes with temperature of the threshold for spike generation have been reported in neocortex (Volgushev et al. 2000b). Both increased input resistance and depolarization increase neuronal responsiveness to inputs with cooling. Action potential amplitude and duration also increase with lowering of temperature in the range that we study here (Thompson et al. 1985; Volgushev et al. 2000b), as well as calcium entry with presynaptic action potentials (Borst and Sakmann 1998). Several of these changes point toward increased network excitability for the lower

temperatures in our range (26–32°C) (Volgushev et al. 2000a,b), although how an increased excitability affects the excitatory/inhibitory balance remains to be explored. On the other hand, synaptic transmission undergoes complex changes with cooling that include an increased delay and decreased reliability with cooling, whereas in the range of temperatures studied here, the amplitude of synaptic potentials remained relatively constant (Hardingham and Larkman 1998; Volgushev et al. 2000a). Therefore the modulation of physiological mechanisms by cooling in the range of temperatures of interest does not unequivocally define how network activity will be affected by temperature.

Enzymatic function—and in particular Na^+/K^+ -ATPase function—decreases with lower temperatures (Esmann and Skou 1988). More generally, cooling decreases the metabolism of the tissue and tends to slow down processes, eventually silencing the cortex. For that reason, cooling is often used to decrease activity of a specific area (Ferster et al. 1996; Malhotra and Lomber 2007; Schiller and Malpeli 1977; Uyeda and Fuster 1967). However, even when it reliably silences the neurons at temperatures $<10^\circ\text{C}$, there is often a halo of cortical hyperexcitability (Volgushev et al. 2000a).

In this study we detected changes with temperature within the range 26–41°C. We found that firing rate during up states is modulated by temperature differently from the (sparse) firing rate during down states: the peak firing rate during up states was strongly modulated by temperature, increasing for higher temperatures and decreasing with cooling (Fig. 4, *A* and *B*), whereas that during down states remained relatively constant (Fig. 4C). As a result the ratio of down/up firing rate increased with cooling, eventually reaching a functional state where the up and down firing periods would become continuous (Supplemental Fig. S3). Given the rate of neuronal depolarization with cooling (1 – 2.2 mV/°C; Volgushev et al. 2000b), a simple calculation reveals that at 30°C neuronal membrane potential would be close to threshold and thus ready to fire with small inputs. The cerebral cortex is a network of recurrently connected excitatory and inhibitory neurons with membrane potentials that at 30–32°C are close to firing threshold. At lower

temperatures, the transition from the down to the up state has a shallow slope (Fig. 5B), given that it is unnecessary to build up a large amount of synaptic activity to bring the neurons in the network above threshold (Bazhenov et al. 2002; Compte et al. 2003). In these conditions the occasional summation of miniature excitatory postsynaptic potentials could start up states (Bazhenov et al. 2002). This random mechanism would support the larger CV of the oscillatory cycle observed at low temperatures (Fig. 4F).

The low firing rates during up states at 30–32°C would not be efficient to recruit activity-dependent potassium channels (Ca^{2+} - and Na^{+} -dependent K^{+} currents) that according to our model (Compte et al. 2003; Sanchez-Vives and McCormick 2000) and that of others (Bazhenov et al. 2002; Hill and Tononi 2005) contribute to end up states. The same would happen with other currents like those mediated by activity-dependent mechanisms such as ATP-dependent K^{+} channels (Cunningham et al. 2006). Low firing rates during up states would lead to a reduced accumulation of Ca^{2+} and Na^{+} in neurons, leading to a poor activation of K^{+} channels in the local network and thus to longer up states and to slower slopes from up to down transitions at lower temperatures.

Neuronal input resistance decreases slightly when temperature increases (Thompson et al. 1985; Volgushev et al. 2000b), membrane values become more hyperpolarized (see preceding text), and therefore neurons no longer reach threshold with very small inputs. Within individual synaptic potentials, the speed of transmitter release controls the rate of rise and the amplitude of individual synaptic potentials (Katz and Miledi 1965). Increasing temperature has been reported to decrease the number of failures and to decrease variability in synaptic transmission, making it more reliable (Hardingham and Larkman 1998), whereas the synaptic delay decreases and paired-pulse facilitation increases (Volgushev et al. 2000a). Cortical activity reverberates in the network until a critical number of neurons is locally recruited such that a new up state is generated. The increase in the down to up transition slope increases with temperature (Fig. 5B), which could result from both the increase in slope of individual synaptic potentials and by faster and more efficient summation of synaptic activity until the threshold in individual neurons is reached and the up state is locally generated. This is reflected in the population in a steeper slope of the firing rates. Higher firing rates during up states at warmer temperatures could build up larger concentrations of intracellular Ca^{2+} and Na^{+} , leading to a more efficient activation of K^{+} currents that would terminate up states earlier and with a faster transition.

Regarding speed of propagation of the wave of activity, there is a moderate increase with temperature, detected in three of five cases. In the remaining two cases the propagation speed did not vary with temperature. This could be unexpected since axonal conduction is known to increase with temperature (5%/deg) (Hodgkin and Katz 1949; Johnson and Olsen 1960). However, propagation of activity in the cortical network also depends on other factors such as excitatory/inhibitory balance, reverberation in the network, and excitability of the network (Compte et al. 2003; Pinto et al. 2005; Sanchez-Vives et al. 2008). The larger excitability of neurons in the lower range of temperatures (Volgushev et al. 2000b) and their closeness to threshold probably could compensate factors like the slower axonal conduction at

cooler temperatures. The balance of opposite factors results in a moderate increase in the propagation speed.

We used a previously published computational model of the slow oscillations (Compte et al. 2003) to explore preliminarily what possible manipulations of cellular and synaptic parameters known to be affected by temperature (see earlier text) could explain our experimental observations. Not surprisingly, we could not find a change in an individual parameter that could consistently explain all the experimental observations. We also found that a large set of combinations of plausible parameter changes could be designed to simulate the data. We thus concluded that further mechanistic insight from the experiment would be necessary to constrain the model. Because of this difficulty in constraining numerous and widely different mechanistic scenarios, we consider that a detailed modeling approach would not be very insightful at this point.

Changes in the temperature in the brain are moderate under normal conditions, although temperature measured in the hippocampus increases by an average of 3.2°C in rats while exploring, through the warming of arterial blood at the muscles (Andersen and Moser 1993); however, in rats in a watermaze it decreases by 5°C, providing sufficient change to decrease the slope of synaptic potentials and to increase their latency. Therefore the activity of the cerebral cortex must also be affected by temperature on a daily basis. An obvious situation in which temperature increases is during fever. Fever is known to increase the chance of epileptic discharges, especially in children. Temperatures in the range of fever increase synchronization in hippocampal slices, leading to epileptic activity (Tancredi et al. 1992; Wu et al. 2001). A decrease in GABAergic transmission has also been described as a consequence of hyperthermia (38.5–40°C) (Qu and Leung 2009), particularly in immature rats. We describe here that the activity during up states becomes more synchronized, in the sense that up states have a steep down to up transition and high firing rates are concentrated in short up states, but epileptiform discharges were not observed. We did observe though a tendency to spreading depression while at >40°C, observing it in nine cases at an average temperature of 41.2°C (data not shown). The relation between increased synchronization and epilepsy is such that cooling has been used to treat epilepsy (Rothman 2009; Rothman et al. 2005), since decreasing temperature from 34 to 21°C reduced synchronization in hippocampal slices (Javedan et al. 2002; Motamedi et al. 2006).

We found that temperature nonmonotonically modulated the amplitude of local field potentials during emergent network activity. The LFP spectral power over the band 5–100 Hz was maximal at physiological temperatures. In addition, when we identified clear spectral peaks in the beta/gamma band, they occurred only at physiological temperatures. Taken together, this is indicative that physiological mechanisms are concertedly tuned to generate large-amplitude synaptic activity fluctuations in the network during normal physiological function. This might be revealing the enhanced broadband synchronization of network activity. Consistent with this, previous experiments have shown that the rapid heating of hippocampal slices from 34°C to fever-range temperatures generates transient gamma-range activity followed by spreading depression (Wu et al. 2001). In our experiments, temperature was changed very slowly and we found that strong broadband fluctuations characterize physiological temperatures, whereas spreading depres-

sion occurred at higher temperatures. The results of Wu et al. (2001) suggest that our strong LFP fluctuations might partly emerge from synchronization in network activity.

Alternatively, the maximal power of the LFP signal at physiological temperatures might result from the tuning of synaptic parameters such as spontaneous release, synaptic reliability, or synaptic efficacy. Then, according to the computational model by Timofeev et al. (2000), changes in spontaneous release should affect the down state of cortical slow oscillations, as our results suggest: down state duration is minimal at physiological temperatures (Fig. 3C). On the other hand, such enhanced synaptic noise might provide an optimal noisy environment for network function. Indeed, theoretical studies with biophysical network models for decision-making processes have proposed that strong random components in noisy inputs to neurons might be a fundamental mechanism for nonlinear cortical processing related to higher cognitive functions (Deco et al. 2009). Our results suggest that up and down states in cortical slices regulated by temperature might be a possible experimental model in which this suggestive role of noise in nonlinear network dynamics can be directly assessed experimentally.

ACKNOWLEDGMENTS

We thank M. Winograd for participation in the preliminary experiments.

GRANTS

This work was supported by the Ministry of Science and Innovation of Spain to M. V. Sanchez-Vives and A. Compte.

REFERENCES

- Aghajanian GK, Rasmussen K. Intracellular studies in the facial nucleus illustrating a simple new method for obtaining viable motoneurons in adult rat brain slices. *Synapse* 3: 331–338, 1989.
- Andersen P, Moser EI. Brain temperature and hippocampal function. *Hippocampus* 5: 491–498, 1995.
- Bazhenov M, Timofeev I, Steriade M, Sejnowski TJ. Model of thalamocortical slow-wave oscillations and transitions to activated states. *J Neurosci* 22: 8691–8704, 2002.
- Borst JG, Sakmann B. Calcium current during a single action potential in a large presynaptic terminal of the rat brainstem. *J Physiol* 506: 143–157, 1998.
- Compte A, Reig R, Descalzo VF, Harvey MA, Puccini GD, Sanchez-Vives MV. Spontaneous high-frequency (10–80 Hz) oscillations during up states in the cerebral cortex in vitro. *J Neurosci* 28: 13828–13844, 2008.
- Compte A, Sanchez-Vives MV, McCormick DA, Wang XJ. Cellular and network mechanisms of slow oscillatory activity (<1 Hz) and wave propagations in a cortical network model. *J Neurophysiol* 89: 2707–2725, 2003.
- Cunningham MO, Pervouchine DD, Racca C, Kopell NJ, Davies CH, Jones RS, Traub RD, Whittington MA. Neuronal metabolism governs cortical network response state. *Proc Natl Acad Sci USA* 103: 5597–5601, 2006.
- Deco G, Rolls ET, Romo R. Stochastic dynamics as a principle of brain function. *Prog Neurobiol* 88: 1–16, 2009.
- Esmann M, Skou JC. Temperature-dependencies of various catalytic activities of membrane-bound Na⁺/K⁺-ATPase from ox brain, ox kidney and shark rectal gland and of C12E8-solubilized shark Na⁺/K⁺-ATPase. *Biochim Biophys Acta* 944: 344–350, 1988.
- Ferster D, Chung S, Wheat H. Orientation selectivity of thalamic input to simple cells of cat visual cortex. *Nature* 380: 249–252, 1996.
- Fujii S, Sasaki H, Ito K, Kaneko K, Kato H. Temperature dependence of synaptic responses in guinea pig hippocampal CA1 neurons in vitro. *Cell Mol Neurobiol* 22: 379–391, 2002.
- Hajos N, Ellender TJ, Zemankovics R, Mann EO, Exley R, Cragg SJ, Freund TF, Paulsen O. Maintaining network activity in submerged hippocampal slices: importance of oxygen supply. *Eur J Neurosci* 29: 319–327, 2009.
- Hardingham NR, Larkman AU. Rapid report: the reliability of excitatory synaptic transmission in slices of rat visual cortex in vitro is temperature dependent. *J Physiol* 507: 249–256, 1998.
- Hill S, Tononi G. Modeling sleep and wakefulness in the thalamocortical system. *J Neurophysiol* 93: 1671–1698, 2005.
- Hodgkin AL, Katz B. The effect of temperature on the electrical activity of the giant axon of the squid. *J Physiol* 109: 240–249, 1949.
- Javedan SP, Fisher RS, Eder HG, Smith K, Wu J. Cooling abolishes neuronal network synchronization in rat hippocampal slices. *Epilepsia* 43: 574–580, 2002.
- Johnson EW, Olsen KJ. Clinical value of motor nerve conduction velocity determination. *J Am Med Assoc* 172: 2030–2035, 1960.
- Kullmann DM, Asztely F. Extrasynaptic glutamate spillover in the hippocampus: evidence and implications. *Trends Neurosci* 21: 8–14, 1998.
- Malhotra S, Lomber SG. Sound localization during homotopic and heterotopic bilateral cooling deactivation of primary and nonprimary auditory cortical areas in the cat. *J Neurophysiol* 97: 26–43, 2007.
- Mattia M, Del Giudice P. Population dynamics of interacting spiking neurons. *Phys Rev E* 66: 1–19, 2002.
- Moser E, Mathiesen I, Andersen P. Association between brain temperature and dentate field potentials in exploring and swimming rats. *Science* 259: 1324–1326, 1993.
- Motamedi GK, Salazar P, Smith EL, Lesser RP, Webber WR, Ortinski PI, Vicini S, Rogawski MA. Termination of epileptiform activity by cooling in rat hippocampal slice epilepsy models. *Epilepsy Res* 70: 200–210, 2006.
- Pinto DJ, Patrick SL, Huang WC, Connors BW. Initiation, propagation, and termination of epileptiform activity in rodent neocortex in vitro involve distinct mechanisms. *J Neurosci* 25: 8131–8140, 2005.
- Qu L, Leung LS. Effects of temperature elevation on neuronal inhibition in hippocampal neurons of immature and mature rats. *J Neurosci Res* 87: 2773–2785, 2009.
- Rothman SM. The therapeutic potential of focal cooling for neocortical epilepsy. *Neurotherapeutics* 6: 251–257, 2009.
- Rothman SM, Smyth MD, Yang XF, Peterson GP. Focal cooling for epilepsy: an alternative therapy that might actually work. *Epilepsy Behav* 7: 214–221, 2005.
- Sanchez-Vives MV, Descalzo VF, Reig R, Figueroa NA, Compte A, Gallego R. Rhythmic spontaneous activity in the piriform cortex. *Cereb Cortex* 18: 1179–1192, 2008.
- Sanchez-Vives MV, McCormick DA. Cellular and network mechanisms of rhythmic recurrent activity in neocortex. *Nat Neurosci* 3: 1027–1034, 2000.
- Schiller PH, Malpeli JG. The effect of striate cortex cooling on area 18 cells in the monkey. *Brain Res* 126: 366–369, 1977.
- Schiller PH, Stryker M, Cynader M, Berman N. Response characteristics of single cells in the monkey superior colliculus following ablation or cooling of visual cortex. *J Neurophysiol* 37: 181–194, 1974.
- Shu Y, Hasenstaub A, McCormick DA. Turning on and off recurrent balanced cortical activity. *Nature* 423: 288–293, 2003.
- Stark E, Abeles M. Predicting movement from multiunit activity. *J Neurosci* 27: 8387–8394, 2007.
- Steriade M, Amzica F, Contreras D. Synchronization of fast (30–40 Hz) spontaneous cortical rhythms during brain activation. *J Neurosci* 16: 392–417, 1996.
- Steriade M, Nunez A, Amzica F. A novel slow (<1 Hz) oscillation of neocortical neurons in vivo: depolarizing and hyperpolarizing components. *J Neurosci* 13: 3252–3265, 1993.
- Tancredi V, D’Arcangelo G, Zona C, Siniscalchi A, Avoli M. Induction of epileptiform activity by temperature elevation in hippocampal slices from young rats: an in vitro model for febrile seizures? *Epilepsia* 33: 228–234, 1992.
- Thompson SM, Masukawa LM, Prince DA. Temperature dependence of intrinsic membrane properties and synaptic potentials in hippocampal CA1 neurons in vitro. *J Neurosci* 5: 817–824, 1985.
- Timofeev I, Grenier F, Bazhenov M, Sejnowski TJ, Steriade M. Origin of slow cortical oscillations in deafferented cortical slabs. *Cereb Cortex* 10: 1185–1199, 2000.
- Uyeda AA, Fuster JM. Effects of cooling “association cortex” on visual evoked potentials. *Psychol Rep* 20: 377–378, 1967.
- Volgushev M, Vidyasagar TR, Chistiakova M, Eysel UT. Synaptic transmission in the neocortex during reversible cooling. *Neuroscience* 98: 9–22, 2000a.
- Volgushev M, Vidyasagar TR, Chistiakova M, Yousef T, Eysel UT. Membrane properties and spike generation in rat visual cortical cells during reversible cooling. *J Physiol* 522: 59–76, 2000b.
- Wu J, Javedan SP, Ellsworth K, Smith K, Fisher RS. Gamma oscillation underlies hyperthermia-induced epileptiform-like spikes in immature rat hippocampal slices (Abstract). *BMC Neurosci* 2: 18, 2001.